Blind Cancellation of Wideband Frequency Modulated Interference in a Wideband Acoustic Communication Channel

J. S. Dhanoa
R. F. Ormondroyd
E. J. Hughes

Department of Aerospace, Power and Sensors
Cranfield University, The Defence Academy of the UK,
Shrivenham, Swindon, SN6 8LA, UK

Abstract - **This paper presents a new method of cancelling wideband interference from digital acoustic communication signals used in underwater communication systems. The interference is from other co-channel acoustic systems, such as navigation systems, that have a bandwidth comparable to the acoustic communication signal. The effectiveness of the new successive interference cancellation algorithm is largely due to a blind interference estimator that uses a multi-objective evolutionary algorithm.**

I. INTRODUCTION

The frequency spectrum available to support underwater acoustic signal transmission is severely limited by noise and dispersion, especially in the littoral environment. This means that the same spectrum has to be shared by systems as diverse as acoustic communication systems and acoustic navigational aides such as echo-sounders and SONAR. Navigational systems frequently use high power, wideband, frequency-modulated signals to achieve long-ranges and high range resolution. Further, improvements in computational power mean that these systems are increasingly using complex waveforms that may change on a pulse-to-pulse basis.

Over a corresponding period of time, considerable progress has been made in the development of high data rate digital acoustic communication systems that require high sensitivity receivers. Consequently, as the numbers of users sharing the underwater channel increase, a situation is arising where there can be high levels of interference between high power navigation systems and high sensitivity communication systems (and *vice versa*).

The problem of interference in the underwater channel has recently been highlighted by Preisig and Johnson [1] who proposed the use of new detection techniques that perform well in the presence of such interference. However, this paper takes a different approach and proposes the use of successive interference cancellation, which could either be used independently or with the detection schemes proposed in [1] to improve the performance of sensitive underwater acoustic digital communication systems in the presence of co-channel, wideband, interference.

One of the earliest methods of acoustic interference cancellation is to use adaptive beamforming whereby a null in the receiving array pattern is placed in the direction of the interference [2]. However, many of the platforms requiring on-board digital acoustic communication systems are small and cannot deploy large arrays for spatial processing. In addition, the wideband nature of the interference precludes the use of simple filtering as a means of interference suppression.

In a recent paper Chen, Hudson and Yao [3] have also highlighted the problem of interference in underwater acoustic channels and the unsuitability of conventional interference cancellation methods such as cepstrum based deconvolution and many methods of interference cancellation often used for RF communication systems. Furthermore, since it is assumed that the parameters of the interfering signal may change on a pulse-to-pulse basis, (either intentionally or due to the rapid time variation of the channel characteristics) this precludes the use of conventional adaptive interference cancellers. In this paper we propose a blind interference cancellation technique that is suitable for the underwater acoustic communication channel.

The aim of the paper is two-fold. First, it shows how a multi-objective evolutionary algorithm (EA) can be used to estimate the waveform of a wideband interfering signal in the presence of noise and the wanted signal. The performance of the new estimator is demonstrated through its mean square error characteristics. Second, it shows how this estimate of the interfering signal can be used in a successive interference cancellation system and the improvement in the performance of a typical underwater acoustic digital communication system. Consequently, the novel feature of this paper is the interference estimation algorithm rather than the method of interference cancellation *per se*.

II. THE NEW INTERFERENCE CANCELLER

Figure 1 shows a block diagram of the successive interference canceller which uses a multi-objective evolutionary algorithm in the interference estimation process. In structure, it is simpler than a traditional adaptive interference canceller, since it is non-adaptive. The new method is effective because it is able to accurately estimate the waveform of the interfering signal on a pulse-to-pulse basis in the presence of other non-Gaussian signals, despite a limited number of samples and limited *a priori* knowledge of the interfering signal waveform. The only *a priori* information required by the estimator is that the interfering signal is represented by an arbitrary non-linear chirp waveform, which encompasses linear chirps and pure sinusoids.

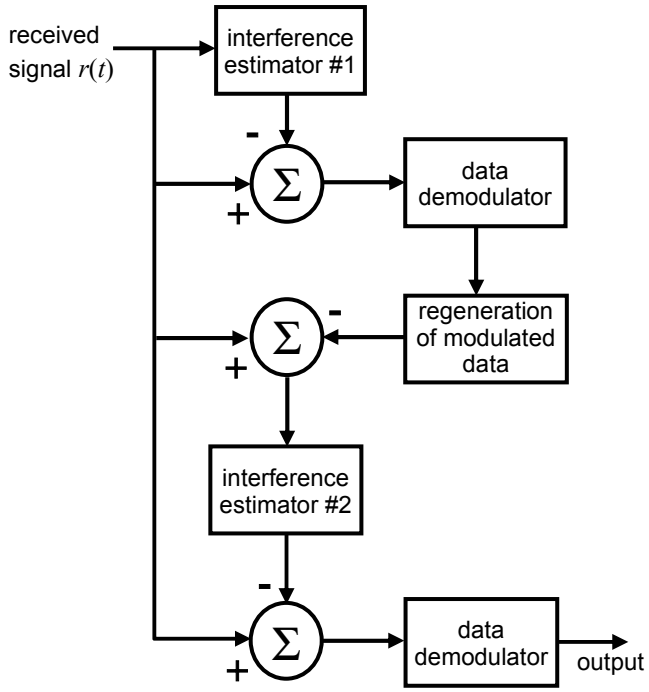

Fig.1 Block diagram of the interference canceller

It is assumed that the 'wanted' signal comprises a wideband digital acoustic signal such as an MPSK or QAM signal [4]:

$$s(t) = A_1(t)\cos(2\pi f_c t + \theta(t)) \tag{1}$$

where $A_1(t)$ is the amplitude of the signal (which may be time-varying for QAM modulation), $f_c(t)$ is the acoustic carrier frequency and $\theta(t)$ is the time varying phase representing the mapping of the symbols on to the carrier phase.

In contrast, the interfering signal (assumed to be a navigation signal) consists of non-linearly frequency-modulated pulses:

$$y(t) = A_2 \sin(2\pi f_i t + \phi) \quad \text{for } 0 \le t \le T_d \tag{2}$$

where A_2 is the amplitude of the interfering signal, ϕ is the initial phase of the interference, T_d is the duration of the interfering pulse and $f_i(t)$ is a non-linearly time-varying frequency whose time variation is expressed as (for example):

$$f_i(t) = f_1 + \sigma t + (f_2 - f_1 - \sigma)t^2 \tag{3}$$

where f_1 and f_2 are the start and stop frequencies respectively, σ is the chirp non-linearity factor and t is the time variable. The received signal is:

$$r(t) = s(t) + y(t) + n(t) \tag{4}$$

where $n(t)$ is additive white Gaussian noise (AWGN). The interfering signal, $y(t)$, has a wide dynamic range and may be stronger than the wanted digital communication signal. In addition, the spectra of the two signals overlap significantly.

As shown in Fig. 1, the received signal is passed to the first interference estimator. The estimator matches both the time-domain waveform of the received signal and its spectrum to a replica signal that represents the interference signal based on the assumption that the interference signal is a chirped waveform. The estimate of the interfering waveform is optimised using a multi-objective EA. The estimated interference waveform is then used to partially remove the interference on the incoming signal. The recovered data is then used in a second stage of interference estimation and cancellation to provide improved performance, as discussed later.

A. Interference estimator

The estimation of the interference signal is based on the use of EAs. The authors have previously used EAs to parameterise linear and non-linear chirps in AWGN [5][6]. However, in this paper, rather than *parameterise* the waveform, we use a multi-objective EA [7] to obtain a *sampled estimate* of the interference waveform in the presence of other, non-Gaussian, signals.

EAs are optimization procedures that operate over a number of cycles (generations). A *population* of M independent individuals is maintained by the algorithm, each individual representing a potential solution to the problem. Each individual has one *chromosome*. This is the genetic description of the solution and may be broken into n sections called *genes*. Each gene represents a single parameter of the problem. In this problem, the chromosome consists of four genes representing: the start frequency, f_1, stop frequency, f_2, the non-linearity factor, σ, and the initial phase, ϕ. However, other parametric descriptions of the chirped interference waveforms could have been used.

The three simple operations found in nature, natural selection, mating and mutation are used to generate new chromosomes and therefore new potential solutions. Each chromosome is evaluated at every generation using an *objective function* that is able to distinguish good solutions from bad ones and score their performance. With each new generation, some of the old population who perform poorly against the objective function are removed to make room for the new offspring if their performance is better. Although there are various optimization techniques available within evolutionary algorithms, we have found Differential Evolution (DE) to be most suitable for this application because of its fast convergence.

B. Differential Evolution

Differential Evolution is an evolutionary technique that generates new chromosomes that are related to the current spatial distribution of the population. This is done by adding the weighted difference between two chromosomes to a third

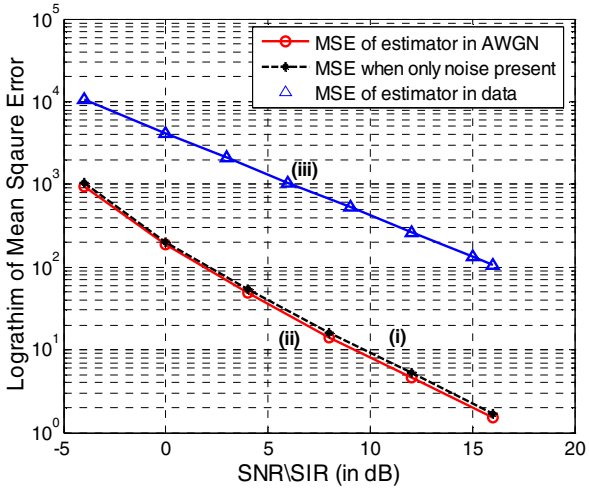

Fig. 2 Graphs of mean square error of the EA-based estimator

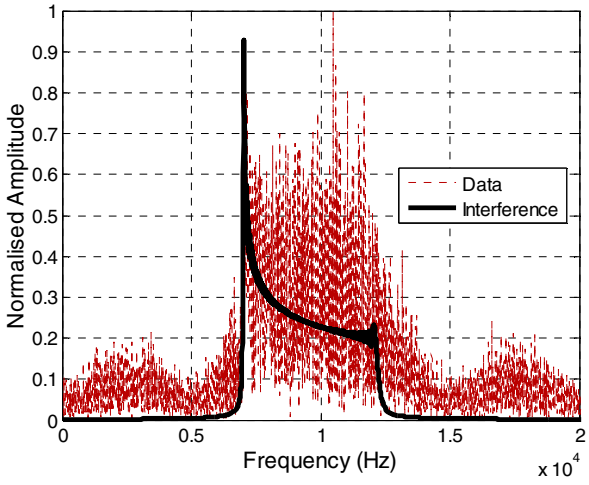

Fig. 3 Spectrum of the data and the interference

chromosome to produce a new chromosome, $\vec{P}_t$ for each member of the population:

$$\vec{P}_t = F\left(\vec{P}_a - \vec{P}_b\right) + \vec{P}_c \tag{5}$$

where chromosomes $\vec{P}_a$, $\vec{P}_b$ and $\vec{P}_c$ are chosen from the population without replacement and F is a scaling factor. The genes of this new chromosome are then crossed with the parent chromosome to generate the child chromosome. The crossover process is controlled by a crossover parameter C. In general, the scaling parameter, F, and the crossover parameter, C, lie in the range [0.5, 1]. The crossover region begins at a randomly chosen parameter in the chromosome and then a segment of length L genes is copied from $\vec{P}_t$ to the parent chromosome to create the child chromosome. If the segment is longer than the remaining length of the chromosome, the segment is wrapped to the beginning of the chromosome.

The length L is chosen probabilistically and is given by:

$$P(L \geq v) = C^{v-1} \quad \text{for } v > 0 \tag{6}$$

The performance of the child chromosome as a possible solution is evaluated using the objective function and if it has a better objective value than the parent, the child chromosome replaces the parent.

C. Objective function

The fitness of a particular chromosome is based on: (a) regenerating the interference waveform from the genes, (b) obtaining its spectrum and (c) comparing the estimated waveform and the received signal in both the time and frequency domains. The basis for the comparison in both domains is the mean square error:

$$E_f = \frac{\sum_{k=1}^{N-1} (Y_k - X_k)^2}{N} \tag{7}$$

$$E_t = \frac{\sum_{k=1}^{M} (y_k - x_k)^2}{M} \tag{8}$$

where E_f and E_t are the mean square errors in frequency and time respectively, Y_k and X_k are the k^{th} spectral components of the received signal, y_k and the regenerated waveform, x_k respectively. M and N represents the number of samples taken and the number of frequency bins used in the spectral estimate, respectively. Often $M = N$, but this need not always be the case. The chromosome giving the least mean square error in either domain is chosen as the best match; i.e.:

$$E = \min\left[E_f, E_t\right] \tag{9}$$

D. MSE performance of the interference estimator

In this section, the performance of the new waveform estimator in AWGN is presented. For this case, a non-linear frequency modulated pulse waveform was used as the trial interference waveform. The parameters for this waveform were: amplitude, $A_2 = 1$ start frequency, $f_1 = 7\text{kHz}$, stop frequency, $f_2 = 14\text{kHz}$ and the chirp non-linearity factor, $\sigma = -30$.

Figure 2 shows the mean square error (MSE) between the spectrum of this test waveform and the estimated waveform under different SNRs. This plot has been obtained as the average MSE of 5 runs at each SNR. Curve (i) (dotted line) shows the contribution to the MSE due to the noise present within the received waveform and curve (ii) shows the MSE between the received and the estimated waveform. In an ideal estimator, the signal should be matched exactly, with the only residual being noise. As can be seen the new estimator is very close to the ideal. However, in the presence

of other non-Gaussian signals (in this case QPSK modulated data representing the digital acoustic communication signal), the performance of the EA interference estimator degrades due to the cross-correlation between the various signal components. This is shown as curve (iii) in Fig. 2 for the situation where the power of the digital communication signal is equal to the power of the interference waveform being estimated. In this case, the overlapping spectra of the two waveforms in the absence of AWGN is shown in Fig. 3.

III SYSTEM PERFORMANCE WITH THE INTERFERENCE CANCELLER

In this section, the performance of the wideband digital acoustic communication system is presented with the new interference canceller for the situation where the communication signal suffers from the interference of the co-channel navigational signal and AWGN. The parameters of the digital acoustic communication system are listed in Table I. The parameters of the non-linear interfering waveform are as given in the previous section. A 'snapshot' of the spectrum of the wanted signal (dotted line) and the interfering signal (solid line) are shown in Fig. 3 and indicate that the two signals do have a similar bandwidth.

TABLE I
SIGNAL PARAMETERS OF THE DIGITAL COMMUNICATION SYSTEM

Carrier frequency	10kHz
Sampling frequency	40kHz
Data rate	5kbaud
Modulation	QPSK
Duration of interference, T_d	0.4352s

Figure 4 shows a scatter graph of the points of the received QPSK constellation before any interference cancellation is applied for the case where the SNR is 10dB. The signal to interference ratio (SIR) of the two signals is 0dB. The corresponding bit error probability of the digital acoustic communication system without interference cancellation is given by curve (i) of Fig. 5 as a function of the additive Gaussian noise. In this case the signal power level and the interference power level are maintained at a constant value and the noise power is varied to vary SNR.. It is clear that at this level of interference mutual co-channel operation of the two systems is impossible and the bit error probability is close to 0.5.

However, after only one iteration of interference cancellation, the constellation of the received QPSK signal, shown in Fig. 6, is considerably improved compared with Fig. 4. As a consequence, the bit error probability performance is substantially improved (as shown by curve (ii) of Fig. 5).

Curve (iii) of Fig. 5 shows the bit error probability curve for the case where there is no interference and the digital acoustic communication system is corrupted only with additive Gaussian noise. It is apparent that although the new interference cancellation system has significantly improved the performance of the digital communication system, to the point where it is now feasible for the two systems to operate co-channel, there is still potential for improvement. It is clear, that the data errors in the communication system for the case of only one iteration of the interference cancellation scheme are due to the inaccuracies in the estimate of the interference waveform at this poor SIR due to the correlation between the data signal and the interference waveform, as shown in Fig. 2. In order to further improve the performance of the blind interference cancellation system, a successive interference strategy was used to reduce the effect of the digital acoustic data signal on the estimate of the interference signal. Referring to Fig. 1, in this approach, the QPSK data symbols are detected after the first iteration of interference cancellation using an appropriate detector. The detected data symbols are

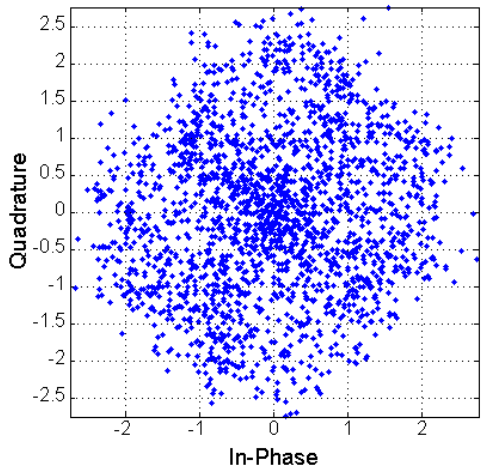

Fig. 4 Scatter plot of the data constellation with the interference at an SNR of 10dB

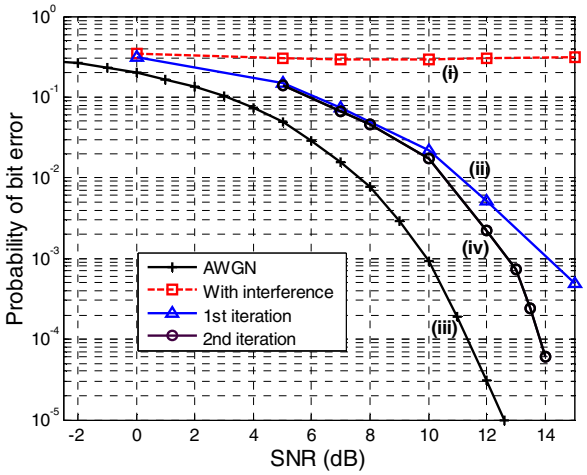

Fig. 5 Bit error probability of the communication system

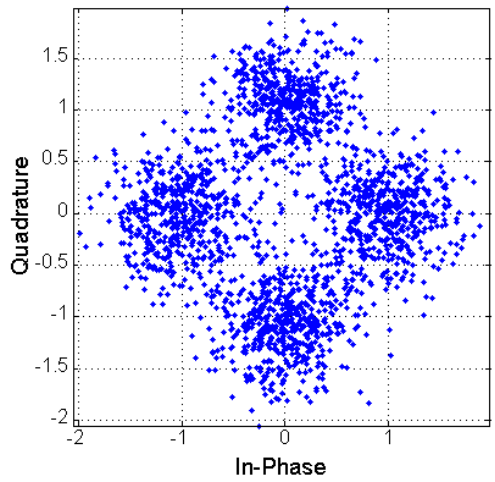

Fig. 6 Scatter plots of the data constellation with interference removed at an SNR of 10dB

then remodulated onto a regenerated carrier and this is used in the second stage of interference estimation to remove the effect of the digital data symbols from the chirped interference signal. This 'cleaner' interference signal is then re-estimated by the EA, and the re-estimate of the interfering signal cancelled from the original received signal. Curve (iv) of Fig. 5 shows the improvement in bit error probability performance. It will be seen that for large SNR, the improved probability in detecting the data symbols at the first iteration gives rise to improved interference estimation, and improved bit error performance at the second iteration. However, when the SNR is poor, the gain in performance reduces.

V CONCLUSIONS

This paper has introduced a new blind wideband interference estimator algorithm based on EAs that can be used in a successive interference cancellation system to minimise the mutual interference between co-channel systems. The performance of the new approach has been demonstrated for an underwater acoustic channel where, due to the limited bandwidth, co-channel interference between low power acoustic communication systems and navigation systems is a potential problem. It has been shown that the new EA interference estimator has almost ideal performance when detecting wideband non-linear chirps in additive Gaussian noise, but that correlation between the two signals reduces its performance. To combat this, a successive interference strategy is used to improve the performance of the communication system by the improving the estimate of the interfering signal.

REFERENCES

[1] J.C. Preisig and M.P. Johnson, "Signal detection for communications in the underwater acoustic environment", *IEEE Journal of Oceanic Engineering*, vol. 26, no. 4, pp. 572-585, 1991.

[2] J. Kesler and S. Haykin, "Adaptive interference canceller using Kalman filtering", *ICASSP '81*, vol 6, pp. 546-549, 1981.

[3] J.C. Chen, R.E. Hudson and Yao Kung, "Fast frequency-domain acoustic channel estimation with interference cancellation", *ICASSP '02*, vol. 2, pp. 1709-1712, 2002.

[4] M. Stojanovic, "Recent advances in high-speed underwater acoustic communications", *IEEE Journal of Oceanic Engineering*, vol. 21, no. 2, pp. 125-136, 1996.

[5] J.S. Dhanoa, E.J. Hughes and R.F. Ormondroyd, "Simultaneous detection and parameter estimation of multiple linear chirps", *ICASSP'03*, vol. 6, pp. 129-132, 2003.

[6] J.S. Dhanoa, E.J. Hughes and R.F. Ormondroyd, "Parametric spectral analysis of multiple non-linear chirps using evolutionary algorithms", *ISSPA'03*, vol. 1 pp. 141-144, 2003.

[7] K. Deb, "*Multi-objective optimisation using evolutionary algorithms*", John Wiley and Sons, 2001.